Supporting Information

Characterization and reuse of SiC flakes generated during electrochemical etching of 4H-SiC wafers

Matteo Barcellona†[a], Vanessa Spanò†[a], Roberto Fiorenza[a], Salvatore Scirè[a], Thomas Defforge[b], Gaël Gautier[b] and Maria Elena Fragalà*[a]

1 University of Catania and Instm Udr Catania, Department of Chemical Sciences, Viale Andrea Doria, 6, 95125 - Catania (Italy)

2 GREMAN UMR-CNRS 7347, INSA Centre Val de Loire, Université de Tours, Tours, France

† Authors equally contributed.

* Corresponding author email : me.fragala@unict.it

1. Methylene blue calibration curve

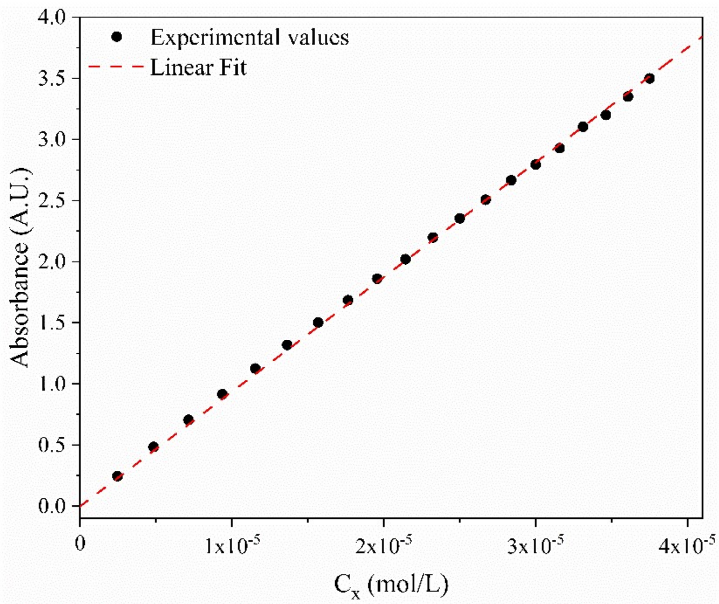

Fig. S1 Linear fit of methylene blue UV-Vis absorbance as a function of molar concentration. The experimental values are reported in black dots. The linear fit is displayed as a dashed red line.

2. Morphological and surface chemical investigations

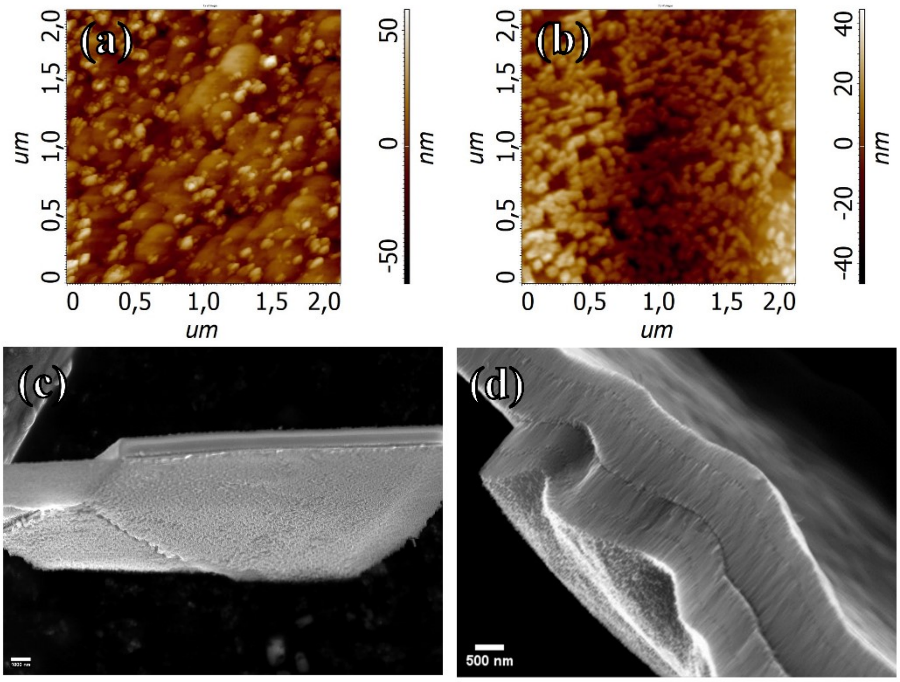

Fig. S2 AFM 2D images of 4H-SiC (a) Si-face and (b) C-face flakes. SEM micrographs of 4H-SiC (c) Si-face and (d) C-face flakes sidewalls.

Tab. S1 XPS surface elemental composition of 4H-SiC reference and 4H-SiC flakes investigated on both Si-face and C-face.

Samples	C%	Si%	O%	F%	C/Si	O/Si
4H-SiC Si-face reference	46.99	41.70	11.05	NA	1.13	0.26
4H-SiC Si-face flakes	47.65	36.49	14.14	1.71	1.31	0.39
4H-SiC C-face reference	36.21	37.87	25.92	NA	0.96	0.68
4H-SiC C-face flakes	44.08	39.59	15.01	1.32	1.11	0.38

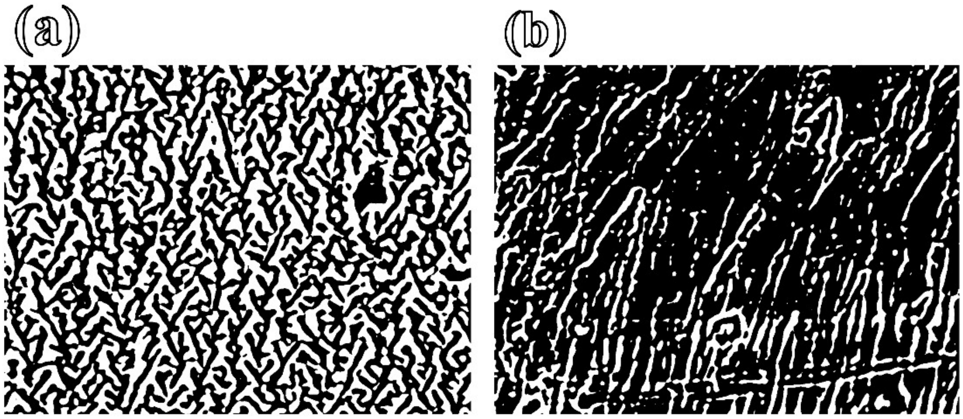

Fig. S3 Threshold image from SEM micrographs of 4H-SiC (a) Si-face and (b) C-face flakes. The pores are highlighted in white whilst the material portion is displayed in black.

Tab. S2 Average pores' size values of Si-face and C-face 4H-SiC flakes by varying the current density and HF concentration.

	Current density (mA/cm^2)	HF concentration (wt%)	Average pores' size (nm)
This work	510	15	Si-face = 4.4 C-face = 59.4
Other formulations	510	↓	Si-face = 23.4 C-face = 31.3
	↓	15	Si-face = 31.8 C-face = 38.7

3. Isotherm adsorption: thermodynamics and kinetics

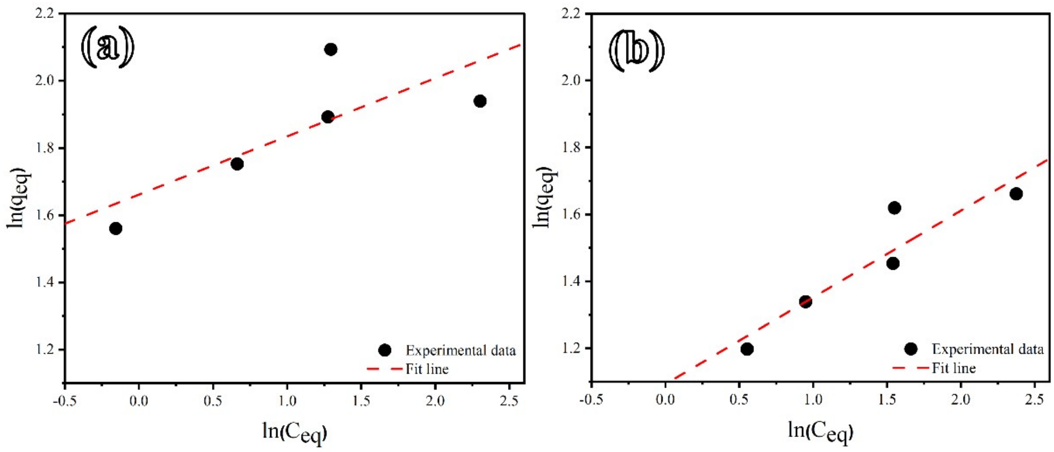

Fig. S4 Freundlich's thermodynamics model plots from MB adsorption isotherm at 7, 10, 15, 25, and 30 µM of 4H-SiC (a) Si-face and (b) C-face flakes adsorbents. The linear fit is shown as red dashed line.

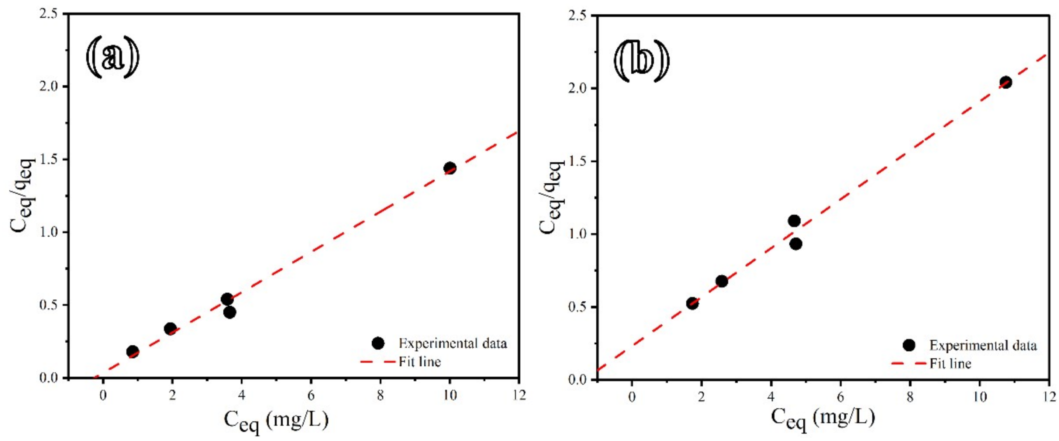

Fig. S5 Langmuir's thermodynamics model plots from MB adsorption isotherm at 7, 10, 15, 25, and 30 μM of 4H-SiC (a) Si-face and (b) C-face flakes adsorbents. The linear fit is shown as red dashed line.

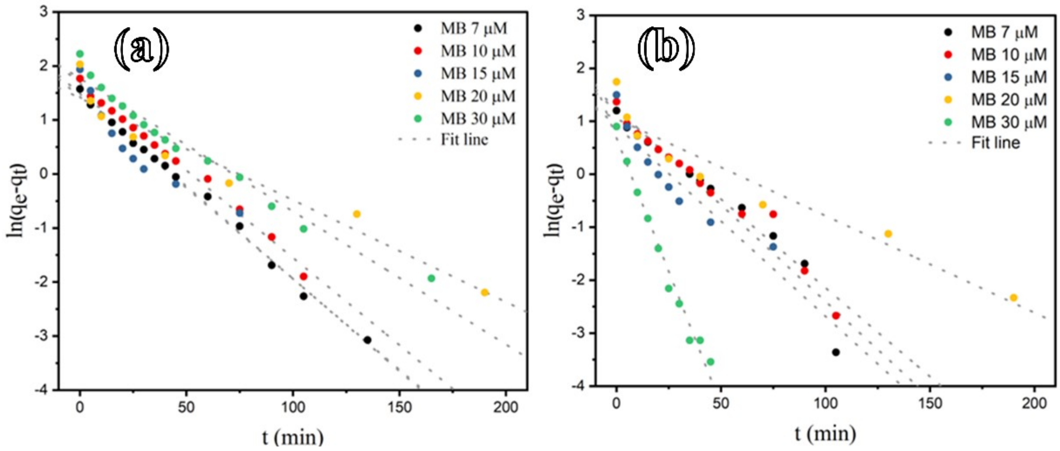

Fig. S6 Pseudo first-order kinetics model from MB adsorption isotherm at 7, 10, 15, 25, and 30 μM of 4H-SiC (a) Si-face and (b) C-face flakes adsorbents.

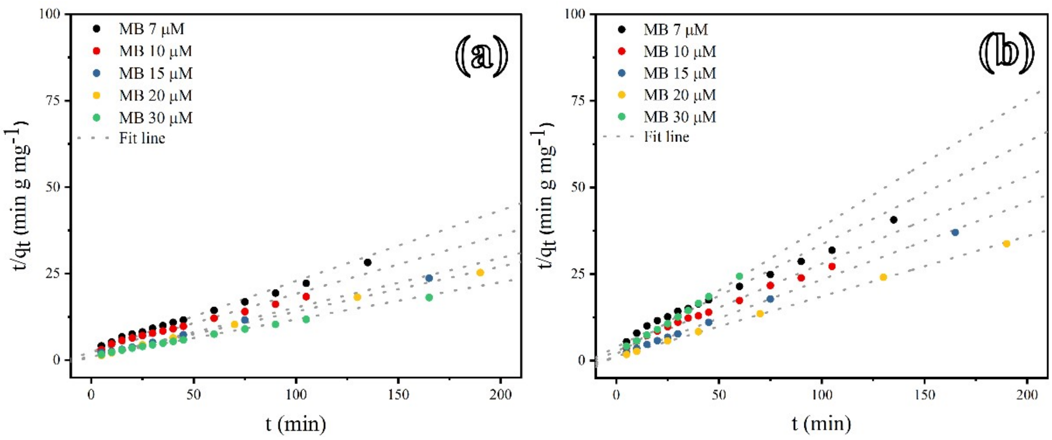

Fig. S7 Pseudo second-order kinetics model from MB adsorption isotherm at 7, 10, 15, 25, and 30 μM of 4H-SiC (a) Si-face and (b) C-face flakes adsorbents.

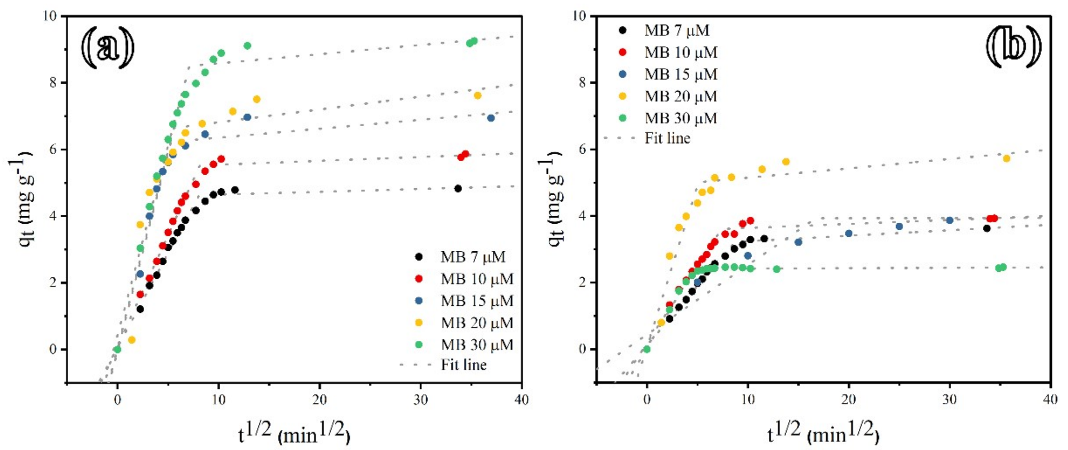

Fig. S8 Weber's kinetics model from MB adsorption isotherm at 7, 10, 15, 25, and 30 μM of 4H-SiC (a) Si-face and (b) C-face flakes adsorbents.

Tab. S3 Parameters of pseudo-first-order, pseudo-second-order, and Weber's models of MB adsorption kinetics at 7, 10, 15, 25, and 30 μM on 4H-SiC Si-face and C-face flakes adsorbents.

Adsorbents	**MB concentrations (μM)**	**Pseudo-first order parameters K_{pf} (min^{-1}), q_e^f (mg g^{-1})**	**R^2**	**Pseudo-second order parameters K_{ps} (g mg^{-1} min^{-1}), q_e^f (mg g^{-1})**	**R^2**	**Intraparticle diffusion parameters K_{i1}, K_{i2} (mg g^{-1} min$^{-1/2}$), q_c (mg g^{-1})**	**R^2**
4H-SiC flakes Si-face	7	K_{pf} =0.079 q_e^f =4.420	0.999	K_{ps}=0.017 q_e^f =4.890	0.999	K_{i1}=0.565 K_{i2}=0.0086 q_c =8.066	0.993
	10	K_{pf}=0.074 q_e^f=5.386	0.999	K_{ps}=0.013 q_e^f=5.887	0.999	K_{i1} =0.666 K_{i2} =0.011 q_c =8.139	0.994
	15	K_{pf} =0.078 q_e^f=4.164	0.999	K_{ps} =0.023 q_e^f=6.980	0.999	K_{i1} =1.184 K_{i2} =0.026 q_c =5.281	0.981

	25	$K_{pf}=0.043$ $q_e^f=4.084$	0.999	$K_{ps}=0.017$ $q_e^f=7.666$	0.999	$K_{i1}=1.183$ $K_{i2}=0.038$ $q_c=5.571$	0.927
	30	$K_{pf}=0.057$ $q_e^f=5.877$	0.997	$K_{ps}=0.011$ $q_e^f=9.298$	0.999	$K_{i1}=1.136$ $K_{i2}=0.027$ $q_c=7.097$	0.986
4H-SiC flakes C-face	7	$K_{pf}=0.084$ $q_e^f=3.458$	0.945	$K_{ps}=0.023$ $q_e^f=3.374$	0.999	$K_{i1}=0.355$ $K_{i2}=0.016$ $q_c=8.728$	0.993
	10	$K_{pf}=0.077$ $q_e^f=3.333$	0.967	$K_{ps}=0.023$ $q_e^f= 3.961$	0.999	$K_{i1}=0.464$ $K_{i2}=0.012$ $q_c=7.366$	0.987

	15	K_{pf}=0.083 q_e^f=2.485	0.870	K_{ps}=0.044 q_e^f=4.490	0.999	K_{i1}=0.208 K_{i2}= 0.0004 q_c=16.731	0.928
	25	K_{pf}=0.042 q_e^f=2.847	0.923	K_{ps}=0.025 q_e^f=5.758	0.999	K_{i1}=0.967 K_{i2}=0.028 q_c=5.104	0.956
	30	K_{pf}=0.232 q_e^f=1.982	0.981	K_{ps}=0.073 q_e^f=2.718	0.997	K_{i1}=0.508 K_{i2}=0.002 q_c=4.670	0.994

4. 4H-SiC flakes recovery

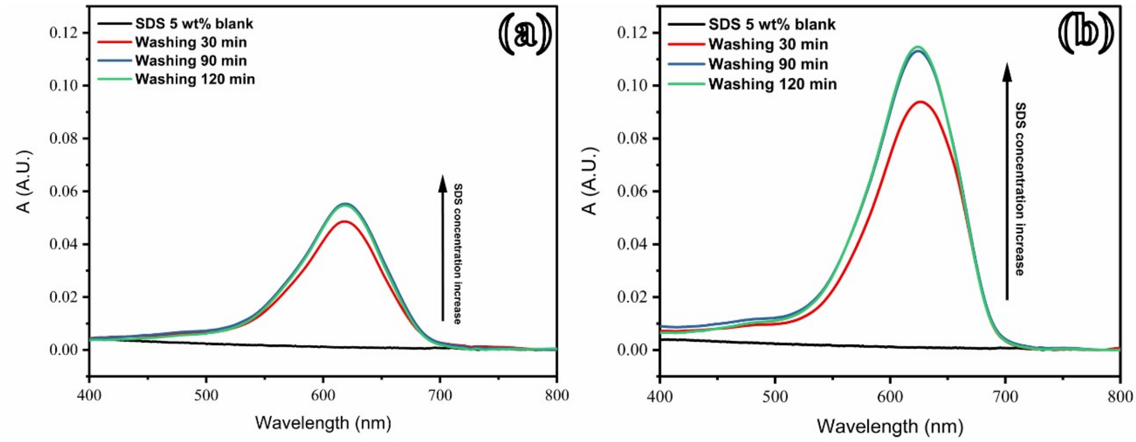

Fig. S9 UV-Vis spectroscopy absorbance of SDS recovery treatment of (a) Si-face and (b) C-face 4H-SiC flakes after MB adsorption saturation.

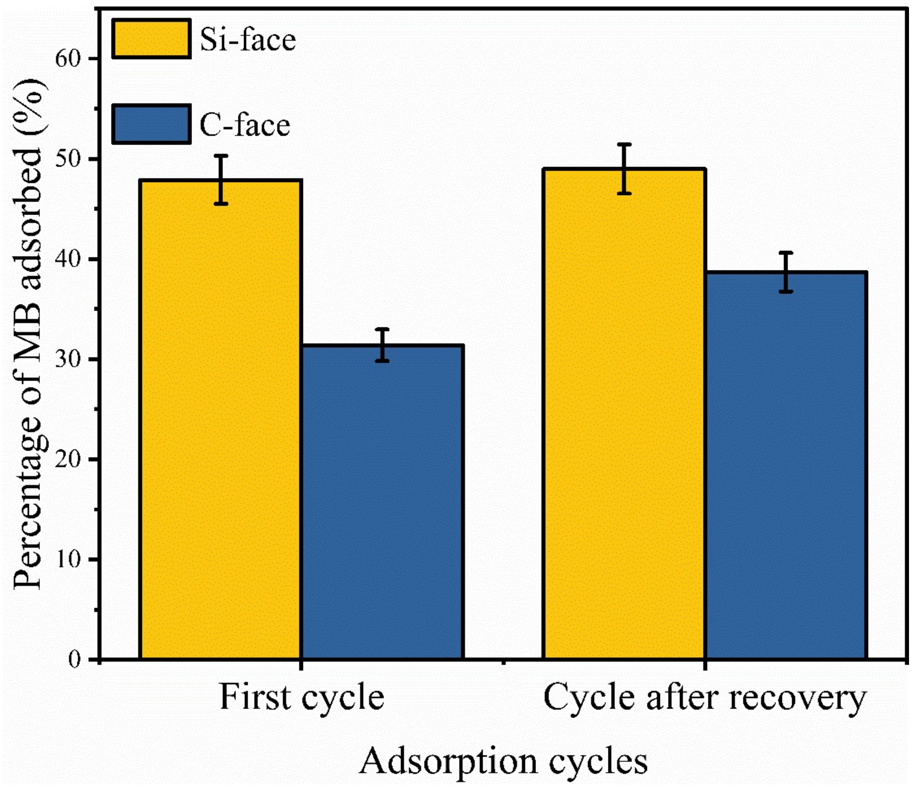

Fig. S10 Bars graph of MB adsorption percentage of Si-face (yellow bars) and C-face (blue bars) flakes before and after recovery performed by HNO_3 70 wt% cleaning treatment.

5. Molecular sieves application

Tab. S4 List of molecules used in the adsorption investigation of porous 4H-SiC flakes. The label "R" refers to complex cycle systems in the dye molecules. The molecular structures are shown in Fig. S11.

Molecules	Molecule length (nm)	M_w (Da)	Charge	Charged chemical group
MO	1.29	304.34	- (pKa = 3.5)[1]	$-R-SO_3^-$
MB	1.24	284.40	+ (pKa = 8.3)[2]	$-R{=}N^+(CH_3)_2 \leftrightarrow -R-S^+-R-$
RhB	1.29	443.57	+ (pKa = 4.2)[3]	$-R{=}N^+(CH_2CH_3)_2$
Rh6G	1.35	443.57	+ (pKa = 6.13)[4]	$-R{=}N^+H(CH_2CH_3)$
TBT	1.10	334.41	+ (fixed)	$-N-N^+(R){=}N-$

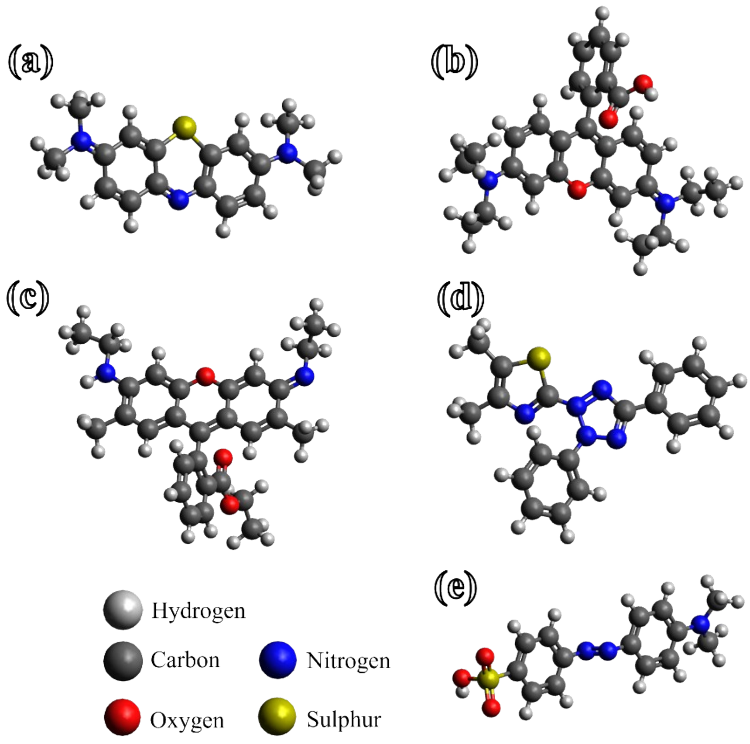

Fig. S11 Molecular structures of (a) Methylene Blue (MB), (b) Rhodamine B (RhB), (c) Rhodamine 6G (Rh6G), (d) Thiazolyl Blue Tetrazolium (TBT), and (e) Methyl Orange (MO).

References

1 R. G. Sandberg, G. H. Henderson, R. D. White and E. M. Eyring, .

2 A. Bensedira, N. Haddaoui, R. Doufnoune, O. Meziane and N. S. Labidi, *Polymers and Polymer Composites*, 2022, **30**, 1–16.

3 R. Zhang, M. Hummelgrd, G. Lv and H. Olin, *Carbon N Y*, 2011, **49**, 1126–1132.

4 S. Rajoriya, S. Bargole and V. K. Saharan, *Ultrason Sonochem*, 2017, **34**, 183–194.